High-Speed Optical Interconnect for Cryogenically Cooled Focal Plane Arrays

Steven Estrella, Dr. Daniel Renner

Freedom Photonics LLC
Santa Barbara, CA 93117
Email: steven@freedomphotonics.com

Takako Hirokawa, Aaron Maharry, Mario Dumont, and Dr. Clint Schow
Electrical & Computer Engineering Department
University of California Santa Barbara
Santa Barbara, CA 93106
Email: schow@ece.ucsb.edu

***Abstract*—Military imaging requirements demand continuous improvements in Focal Plane Array (FPA) resolution, size, sensitivity and frame rate, driving the need for high-speed interconnects between the FPA, located inside a cryogenic Dewar, to the processing electronics in the ambient environment. Significant advances in operational bandwidth are needed to support future high definition (HD) and high-pixel count formats, in addition to faster frame rate requirements (up to a kHz or more). Therefore, interconnect speeds of many tens of Gbps will soon be required with future demand growing to possibly many hundreds of Gbps. Currently, electrical interconnects, which are limited to data rates of ~2.5 Gbps, are used to read-out FPAs. As the number of high-speed metallic interconnect data lines increases, passive thermal heat loading between the cold FPA and the warm Dewar increases, degrading the cryostat cooling efficiency. Optical interconnects, based on either Free-Space Optical (FSO) or fiber-optic link technology, provide a unique solution by significantly minimizing passive heat loading, while simultaneously providing high-speed and scalable interconnects, especially when utilizing wavelength division multiplexing (WDM). Recently, Freedom Photonics LLC and the University of California Santa Barbara, have developed a high-speed optical interconnect for cryogenically cooled FPAs based on a micro-ring resonator electro-optic modulator (EOM) implemented in a silicon (Si) photonics platform, that is WDM scalable for applications requiring >40 Gbps operation. The modulator device, fabricated through the American Institute for Manufacturing (AIM) Photonics program, demonstrated 1E-10 bit error rate (BER) at 10 Gbps and 300 K operation. Subsequent device design iterations have targeted larger bandwidths and mitigation of carrier-freeze out under cryogenic operation utilizing highly doped regions. Progress toward operation at a cryogenic temperature of 77 K, and potentially lower, is reported with promising initial results.**

Keywords—Optical interconnects; Silicon photonics; Cryogenic; Focal plane array

This work was sponsored by the Army Research Office (ARO).
DISTRIBUTION STATEMENT A. Approved for public release.

I. Introduction

Recently, there has been significant interest in high-speed and low-power consumption optical interconnects for various applications, including intra-datacenter communications [1], high-performance computing (HPC) [2], superconducting computing [3], and military imaging. Some applications, such as in high-pixel count and fast frame rate infrared (IR) focal plane arrays (FPA), require operation at cryogenic temperatures and produce data streams of many Gbps that must be read out with low bit error rate. Typically, a metallic interconnect in the form of coaxial cable is used to read out data from the cold environment to the outside ambient environment, however increasing data rates and excessive heat loading necessitate a better solution. An optical interconnect, based on either fiber-optic cable or free-space, provides a very high-speed interconnect with minimal heat loading, capable of 10s of Gbps data rates per channel. Furthermore, through techniques such as wavelength division multiplexing (WDM), total throughput can reach up to 100s of Gbps. Utilizing low-power consumption ring resonator modulators (RRM), implemented in the Si photonics platform available through AIM Photonics, an optical interconnect capable of 10 Gbps and BER < 1E-10 has been demonstrated at room temperature.

II. Optical Interconnect Design

The optical interconnect is designed to be WDM scalable, whereby each WDM channel corresponds to one electrical output from the ROIC. For increased data capacity and throughput, multiple ring resonator modulators can be placed on the common input bus waveguide, whereby each modulator corresponds to and can be addressed by a specific optical wavelength channel. In remoting the optical modulator portion of the optical interconnect in the cryogenic environment, significant savings in cooling power and efficiency can be achieved. Recently, a Si based photonic disk modulator has been demonstrated at cryogenic temperatures [4], highlighting the challenges and possible solutions for such devices.

A conceptual schematic of a WDM scalable high-speed optical interconnect for cryogenically cooled FPAs is shown in Fig. 1. Multiple continuous-wave (CW) lasers can be optically multiplexed (Mux) together onto a single optical channel, either optical fiber or free-space, and couple through the cryostat via an appropriate optical vacuum port and into the Si photonic chip.

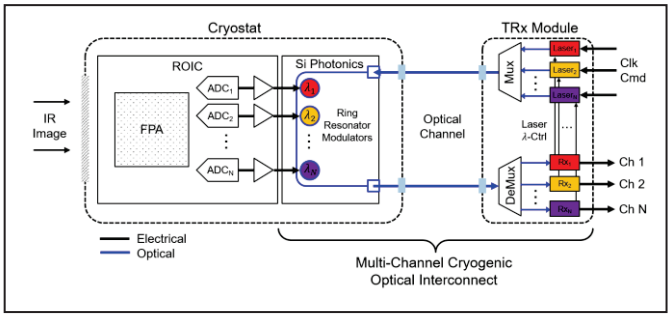

Fig. 1. Conceptual schematic of a WDM scalable, multi-channel cryogenic optical interconnect, whereby output electrical signals from the ROIC modulate incoming CW light from the ambient environment via Si photonic based ring resonator modulators, which are then received in the ambient environment for further signal processing.

In the case of an optical fiber-based channel, either edge or grating based couplers can be used to couple light in and out of the device, with losses on the order of 1.5 to 3 dB at each coupling interface, respectively. For a free-space optical channel, a single 2-D grating coupler can be used as the input and output, whereby polarization is used to differentiate the two directions and to suppress interference and cross-talk. Small footprint (e.g. ~10 μm radius) ring resonator modulators are optically coupled to a common bus waveguide, which routes the input and output light to the appropriate coupler positioned on the device. The analog signals from the FPA are first digitized via analog-to-digital converters (ADC) and then amplified to standard integrated circuit (IC) logic levels in the ROIC, which are then used to modulate the Si RRM devices. The optical signals are then routed out to an optical demultiplexer (DeMux), separating out each WDM channel, before entering an optical receiver and converted back to electrical signals for further signal processing and image formation.

The Si RRM device is based on a lateral Si *p-n* junction (~400 nm wide) on top of a buried oxide (BOX) layer, which also forms an optical waveguide. The *p*- and *n*-contact regions are displaced away from the optical waveguide region (~1.6 μm) so as to not induce additional loss via free-carrier absorption (FCA). Optical modulation is achieved by applying a reverse bias voltage across the *p-n* junction, which causes a change in the refractive index via carrier depletion, and therefore the resonant wavelength of the ring cavity. Placing a laser source at an appropriate point on the Si RRM transmission function will induce amplitude modulation corresponding to the RF input signal. The RF electrical-to-optical (E/O) bandwidth of the Si RRM is determined by both the electrical RC parasitic time-constant and cavity photon lifetime constant. For such small devices, the RC parasitics are very small, and the photon lifetime dominates the bandwidth. The photon lifetime is also directly proportional to the cavity quality factor, Q, which determines the maximum achievable extinction ratio (ER), or contrast between the digital '1' and '0' states. Thus, a trade-off in modulator performance exists between the Si RRM extinction ratio (ER) and RF bandwidth, assuming the device is photon-lifetime limited, which is illustrated by the simulation in Fig. 2. A high Q or ER would allow for small modulation voltages, which is preferred to maintain compatibility with an ROIC.

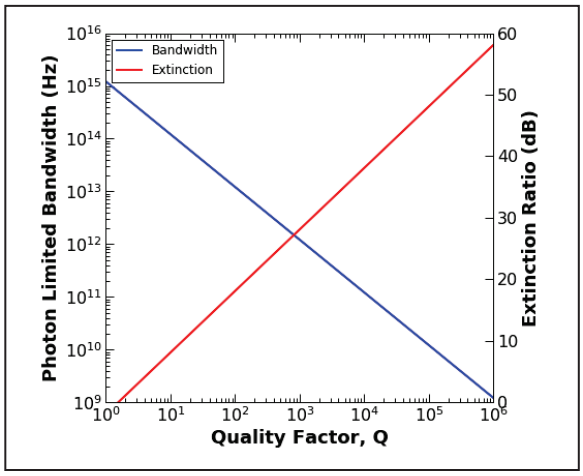

Fig. 2. Photon lifetime limited electrocal-to-optical bandwidth and extinction ratio as a function of ring resonator modulator quality factor, Q.

III. Results and Discussion

The Si RRM device reported here was fabricated through the first offered AIM Photonics fabrication process run. To determine the free-spectral range of the modulator, an external cavity tunable laser was fiber-coupled to the device, and was swept from 1530 nm to 1560 nm, with the optical output power coupled into calibrated power. The spectral response of the device is shown in Fig. 3, with a measured FSR of ~6 nm, allowing for the possibility of multiple WDM channels within the optical C-band. The ripple in the measurement is believed to be caused by optical reflections between the edges of the Si chip. Also, due to the finite number of wavelength points used to measure the spectral response, the ER is believed to be better than 20 dB across the C-band.

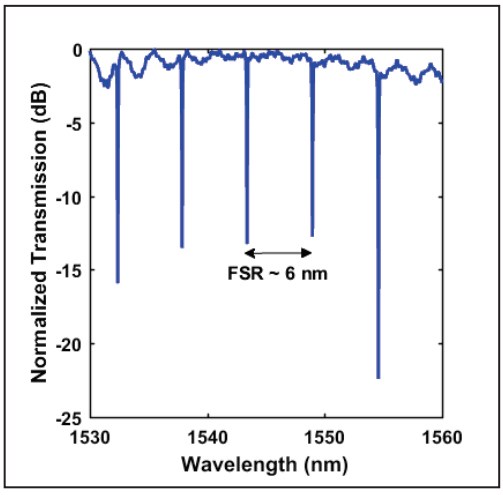

Fig. 3. Normalized transmission DC spectral response of the Si ring resonator modulator from 1530 nm to 1560 nm, with a measured free-spectral range (FSR) of ~6 nm. Spectral response was take at a DC bias voltage of 0.75 V.

To characterize the tuning performance, the Si RRM DC bias voltage dependent spectral response was measured and is shown in Fig. 4. The DC bias voltage range was from 0.75 V to -5 V, which demonstrates the wavelength tuning efficiency in the

forward and reverse bias regions. Due to the diode behavior of the p-n junction, the tuning efficiency increases significantly around the diode turn-on voltage, which can be attributed to the stronger change in refractive index due to carrier injection. In addition to a shift in wavelength resonance with decreasing bias voltage, there is a noticeable change in the ER, which can be attributed to loss via FCA. Through both electrical and spectral characterization of the Si RRM, the RC time and photon lifetime constants were extracted, indicating a photon lifetime-limited small-signal E/O bandwidth of ~20 GHz.

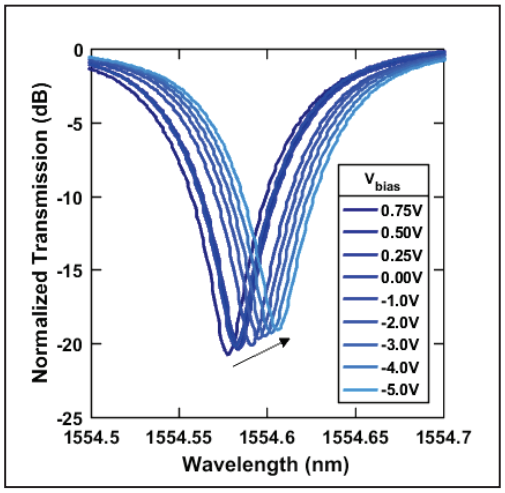

Fig. 4. Normalized transmission DC spectral response of the Si ring resonator modulator as a function of DC bias voltage, V_{bias}, over a 0.2 nm span. The arrow indicates the shifting transmission function toward longer wavelengths and decreasing extinction ratio with decreasing bias voltage.

For room temperature demonstration of the FSO channel concept, a polarization-multiplexed, bi-directional link was constructed using commercial off-the-shelf (COTS) components, while the Si RRM was demonstrated in a laboratory environment at room temperature with fiber-optic cable edge-coupling, shown in Fig. 5. In this manner, the performance of the FSO link and Si RRM device could be independently demonstrated. As illustrated, the input polarization of the CW light is collimated into a ~4 mm diameter beam and set to transverse-electric (TE) polarization before entering the first polarization beam splitter (PBS). The collimated beam propagates a few centimeters before entering the second PBS, and couples into optical fiber via focusing lens. The TE light then enters a COTS $LiNbO_3$ Mach-Zehnder modulator (MZM), where a high-speed pattern generator provides the RF modulation signal. The modulated light then reenters the second PBS after rotating the polarization to transverse magnetic (TM), thereby reflecting the light by 90° back through the FSO channel. The light then reflects off the first PBS, and is coupled into fiber via focusing lens, and converted back to an electrical signal via optical receiver and sent into a digital error analyzer.

The Si RRM was demonstrated in a laboratory environment at room temperature, utilizing edge coupling via optical fiber. An external cavity tunable laser was coupled to an erbium doped fiber amplifier (EDFA) to boost the signal and overcome losses associated with optical coupling. A high-speed pattern generator was used to generate the input electrical signal, which was further amplified using a 26-dB gain broadband amplifier. An RF coaxial cable connected the amplifier output to a high bandwidth G-S style RF probe. A 3-dB attenuator and bias-tee were connected prior to the RF probe, to help suppress electrical reflections and provide DC bias on the RF signal, respectively. The output optical signal from the modulator was sent into an optical receiver, and the resulting electrical signal into a digital error analyzer.

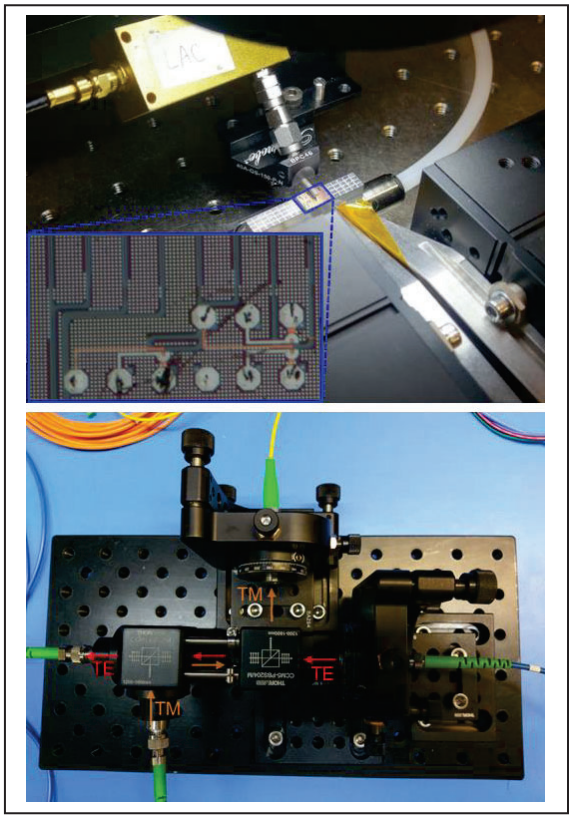

Fig. 5. (Top) Dual fiber edge-coupled Si RRM device under test at UCSB, with an inset microscope image. (Bottom) Prototype bi-directional, polarization-multiplexed FSO system, whereby unmodulated and modulated light are TE and TM polarized, respectively.

Due to the constraints of the pattern generator and broadband amplifier, the amplitude and DC bias of the input electrical signal caused the device to enter the forward bias regime, in order to generate an appreciably high ER. The use of forward bias drive voltage (i.e. carrier injection), caused the bandwidth of the Si RRM to be ultimately RC time-constant limited; therefore, pre-emphasis of the drive signal was utilized to emphasize the high-frequency content of the drive waveform, resulting in appropriate output optical waveforms. Pre-emphasis of the electrical signal was achieved by combining two output electrical channels from the pattern generator, with a variable time delay between the two signals. The corresponding input electrical waveforms and resulting output optical waveforms are shown in Fig. 6, in the form of eye diagrams. Significant enhancement of the beginning of each bit and transition is noticeable, which pre-emphasizes the high frequency content of the signal, which experiences a larger amount of loss through the device.

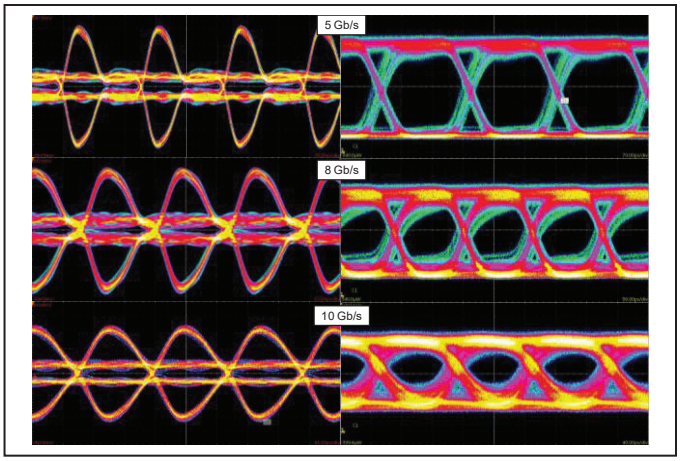

Fig. 6. (Left) Input electrical eye-diamgram waveforms after pre-emphasis, and (right) resulting output electrical waveforms from the Si RRM as a function of data rate, for 5, 8 and 10 Gbps from top to bottom.

The use of pre-emphasis in drive signals for optical interconnects has been shown to improve performance up to 18 Gbps [5] for a forward-biased, current-injected Si RRM. However, there is a penalty in consumed power of the required equalization integrated circuit components, even though energy efficiency of 1.8 pJ/bit at 8 Gbps has been demonstrated in a monolithically integrated CMOS transmitter, utilizing a forward-biased Si RRM [5]. Although the design and implementation of such feed-forward equalization or pre-emphasis circuits is straightforward in many of the Si Photonics platforms, the added power consumption may prohibit its use in certain applications, particularly when used in cryostat at 4 K where thermal dissipation and leakage must be minimized. Therefore, the design and demonstration of Si RRM for carrier depletion mode of operation (i.e. reverse bias regime) is the preferred target goal, as such a design will result in the lowest possible energy consumption, approaching 10 to 100 fJ/bit at data rates of 10 Gbps.

The bit error rate (BER) of the FSO portion of the link and of the Si RRM were separately characterized by Freedom Photonics and UCSB, respectively. The BER vs. the average received optical power was characterized at data rates of 5, 8 and 10 Gbps using a $2^{31} - 1$ PRBS sequence and NRZ-OOK modulation encoding, shown in Fig. 7. Both components of the full system link exhibit BER $\leq$ 1E-10 at data rates up to 10 Gbps, utilizing commercially available laser source and optical receiver components. Reasonable power levels are required at the receiver, implying that laser sources with moderate output power levels (e.g. 10 mW) can be utilized in the full system at cryogenic temperatures.

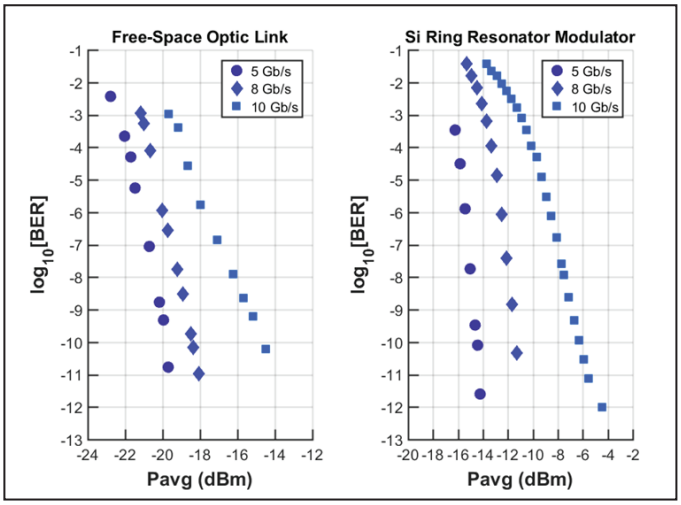

Fig. 7. BER vs. receieved optical power at 5, 8 and 10 Gbps at ~1550 nm (left) for the FSO link and (right) for the Si RRM, both using 2^{31}-1 PRBS NRZ-OOK and achieving BER < 1E-10.

IV. Conclusion

A high-speed optical interconnect for cryogenically cooled FPAs has been designed and demonstrated at room temperature, utilizing a fiber coupled Si RRM. A BER < 1E-10 was achieved at 10 Gbps at room temperature for both the prototype FSO link and Si RRM device. Future work will expand on device operation at cryogenic temperatures.

Acknowledgment

The authors would like to acknowledge Dr. Michael Gerhold of ARO, Dr. Jason Zeibel and Dr. Peter Smith of Army NVESD for insightful discussions. Additionally, we would like to acknowledge funding received from ARO (SBIR Contract No. W911NF-18-C-0096).

References

[1] Kachris, Christoforos, and Ioannis Tomkos. "A survey on optical interconnects for data centers." IEEE Communications Surveys & Tutorials 14.4 (2012): 1021-1036.

[2] Biberman, Aleksandr, and Keren Bergman. "Optical interconnection networks for high-performance computing systems." Reports on Progress in Physics 75.4 (2012).

[3] Holmes, D. Scott, Andrew L. Ripple, and Marc A. Manheimer. "Energy-efficient superconducting computing—Power budgets and requirements." IEEE Transactions on Applied Superconductivity 23.3 (2013).

[4] Gehl, Michael, et al. "Operation of high-speed silicon photonic micro-disk modulators at cryogenic temperatures." Optica 4.3 (2017): 374-382.

[5] Manipatruni, Sasikanth, et al. "High speed carrier injection 18 Gb/s silicon micro-ring electro-optic modulator." Lasers and Electro-Optics Society, 2007. LEOS 2007. The 20th Annual Meeting of the IEEE. IEEE, 2007.

[6] Rosenberg, J., et al. "Ultra-low-voltage micro-ring modulator integrated with a CMOS feed-forward equalization driver," Optical Fiber Communication (OFC) Conference 2011, paper OWQ4, Los Angeles, CA, Mar. 2011.